Amide proton exchange in proteins by EXI kinetics: Studies on the basic pancreatic trypsin inhibitor at variable pH and temperature

ARTICLE *in* BIOCHEMISTRY · JANUARY 1986

Impact Factor: 3.02 · DOI: 10.1021/bi00346a055 · Source: PubMed

3 AUTHORS:

Heinrich Roder
Fox Chase Cancer Center
121 PUBLICATIONS **8,429** CITATIONS
SEE PROFILE

Gerhard Wagner
Harvard Medical School
520 PUBLICATIONS **34,941** CITATIONS
SEE PROFILE

Kurt Wüthrich
The Scripps Research Institute
742 PUBLICATIONS **75,324** CITATIONS
SEE PROFILE

Amide Proton Exchange in Proteins by EX_1 Kinetics: Studies of the Basic Pancreatic Trypsin Inhibitor at Variable p^2H and Temperature†

Heinrich Roder,‡ Gerhard Wagner,* and Kurt Wüthrich
Institut für Molekularbiologie und Biophysik, Eidgenössische Technische Hochschule, Zürich-Hönggerberg, CH-8093 Zürich, Switzerland

Received December 20, 1984

ABSTRACT: With the use of one-dimensional ^1H nuclear magnetic resonance, two-dimensional correlated spectroscopy, and two-dimensional nuclear Overhauser enhancement spectroscopy, the exchange mechanisms for numerous individual amide protons in the basic pancreatic trypsin inhibitor (BPTI) were investigated over a wide range of p^2H and temperature. Correlated exchange under an EX_1 regime was observed only for the most slowly exchanging protons in the central hydrogen bonds of the antiparallel β-sheet and only over a narrow range of temperature and p^2H, i.e., above ca. 55 °C and between p^2H 7 and 9, where the opening rates of the structure fluctuations which promote the exchange of these protons are of the order 0.1 min^{-1}. At p^2H below 7, the exchange of this most stable group of protons is uncorrelated and is governed by an EX_2 mechanism. At p^2H above 9, the exchange is also uncorrelated and occurs via either EX_2 or EX_1 processes promoted by strictly local structure fluctuations. For all other backbone amide protons in BPTI, the exchange was found to be uncorrelated and by an EX_2 mechanism under all conditions of p^2H and temperature where quantitative measurements could be obtained with the methods used, i.e., for $k_{ex} \lesssim 5$ min^{-1}. From these observations with BPTI it can be concluded that the amide proton exchange in globular proteins is quite generally via EX_2 processes, with rare exceptions for measurements with extremely stable protons at high temperature and basic p^2H. This emphasizes the need for further development of suitable concepts for the structural interpretation of EX_2 amide proton exchange [Wagner, G. (1983) *Q. Rev. Biophys. 16*, 1–57; Wagner, G., Stassinopoulou, C. I., & Wüthrich, K. (1984) *Eur. J. Biochem. 145*, 431–436] and for more detailed investigations of the intrinsic exchange rates for solvent-exposed amide protons in the "open" states of a protein [Roder, H., Wagner, G., & Wüthrich, K. (1985) *Biochemistry* (following paper in this issue)].

Among the numerous methods used to probe the dynamic nature of protein structures [e.g., see Gurd & Rothgeb (1979) and Wüthrich & Wagner (1984)], measurements of amide proton exchange rates have for a long time occupied a prominent position (Hvidt & Nielsen, 1966; Englander et al., 1972; Woodward & Hilton, 1979; Wagner & Wüthrich, 1979a; Barksdale & Rosenberg, 1982; Englander & Kallenbach, 1984). A major advance in experimental studies of proton exchange kinetics was achieved with the use of modern high-resolution nuclear magnetic resonance (NMR)[1] experiments. The power of NMR relies on the fact that separate resonance lines can be observed for the individual amide protons. For small proteins, essentially complete assignments for all polypeptide backbone amide protons can be obtained (Wagner & Wüthrich, 1982a; Strop et al., 1983), and therefore, specified amide proton exchange rates can be attributed to particular amino acid residues in the sequence. When the three-dimensional structure is known, a map of amide proton exchange rates across the protein can thus be obtained (Wagner & Wüthrich, 1982b; Wüthrich et al., 1984). BPTI is a small protein which was extensively studied with NMR (Richarz et al., 1979; Wagner & Wüthrich, 1979a; Hilton & Woodward, 1979) and for which a detailed map of amide proton exchange rates was obtained (Wagner & Wüthrich, 1982b).

Somewhat in contrast to the rapid progress made recently with the experimental measurements of amide proton exchange, the details of the mechanism of NH exchange in proteins and quantitative correlations between exchange kinetics and internal mobility are still controversial (Wüthrich et al., 1980; Hilton et al., 1981; Englander & Kallenbach, 1983). As a consequence, it is highly doubtful that the information contained in the experimental data has been fully exploited. In the present paper, we investigate mechanistic aspects of the proton exchange in BPTI on the basis of new experiments. These include studies of NOE's in partially exchanged BPTI samples, which provide direct evidence on the cooperativity of the exchange for neighboring amide protons in the spatial structure of the protein (Wagner, 1980, 1983). Furthermore, quench techniques are employed to extend the use of NMR measurements of individual proton exchange rates to the faster rates encountered at high temperatures, at high p^2H, and after the addition of denaturants.

Fundamental Considerations on Cooperative Proton Exchange

We interpret the exchange kinetics of interior amide protons in globular proteins within the framework of the "breathing model" (Hvidt & Nielsen, 1966; Englander et al., 1972; Wagner & Wüthrich, 1979a; Englander & Kallenbach, 1984). The exchange of an interior proton against a deuteron of the solvent can be described by the scheme:

† This work was supported by the Swiss National Science Foundation (Projects 3.528.79 and 3.284.82).

‡ Present address: Department of Biochemistry and Biophysics, University of Pennsylvania School of Medicine, Philadelphia, PA 19104.

[1] Abbreviations: BPTI, basic pancreatic trypsin inhibitor; TRAM-BPTI, chemical modification of BPTI obtained by transamination of the N-terminus; Gdn·HCl, guanidine hydrochloride; NMR, nuclear magnetic resonance; NOE, nuclear Overhauser effect; NOESY, two-dimensional nuclear Overhauser enhancement spectroscopy; COSY, two-dimensional correlated spectroscopy.

0006-2960/85/0424-7396$01.50/0

$$N(H) \underset{k_2}{\overset{k_1}{\rightleftharpoons}} O(H) \xrightarrow[^2H_2O]{k_3} O(D) \underset{k_1}{\overset{k_2}{\rightleftharpoons}} N(D) \qquad (1)$$

N describes the ensemble of protein conformations in which the proton under consideration is protected from the solvent, and O stands for all conformations in which the proton is exposed to the solvent. In this general scheme, the N(H) to O(H) transition is characterized only to the extent that it leads to solvent exposure of the amide proton, which can be the result of, for example, local structure fluctuations in the folded protein or cooperative unfolding of larger portions of the molecule. The equilibrium between the two classes of states is described by an "opening rate" k_1 and a "closing rate" k_2. We assume that in the open states the proton exchanges with deuterium of the solvent ^2H_2O with the intrinsic exchange rate k_3. Values for individual k_3's can be computed with the rules by Molday et al. (1972) and have also been obtained directly by ^1H NMR exchange measurements in thermally unfolded BPTI (Roder et al., 1985). Under conditions favoring the folded states, i.e., $k_2 >> k_1$, the observed exchange rate, k_{ex}, is given by

$$k_{ex} = \frac{k_1 k_3}{k_2 + k_3} \qquad (2)$$

Depending on the ratio of k_2 to k_3, one may encounter the following two limiting situations (Hvidt & Nielsen, 1966): (i) If $k_2 << k_3$ ("EX_1 limit"), each opening fluctuation leads to an isotope exchange, and eq 2 simplifies to

$$k_{ex} = k_1 \qquad (3)$$

In this case, the exchange is limited by the opening rate k_1. Obviously, NH exchange measurements under EX_1 conditions provide readily interpretable data which can be correlated with a key feature of internal protein motility. (ii) If $k_2 >> k_3$ ("EX_2 limit"), the intrinsic exchange is the rate-limiting step, and eq 2 reduces to

$$k_{ex} = (k_1/k_2)k_3 = Kk_3 \qquad (4)$$

$K = k_1/k_2$ is the equilibrium constant for the conformational transition between the states O and N. In contrast to measurements of k_{ex} under an EX_1 regime, k_{ex} resulting from an EX_2 process is not directly related to a kinetic process in the protein. However, provided that reliable values for k_3 are available (Roder et al., 1985), such experiments can be used to study the equilibria between O and N states for individual amide protons (Wagner et al., 1984).

Since in the EX_2 limit the protein must undergo many opening transitions before a particular proton is exchanged, the exchange of neighboring protons is expected to be uncorrelated, independent of the nature of the opening fluctuations. Information on the cooperativity of the dynamic processes can thus only be gained in the EX_1 limit, where the opening process is directly observed, and demonstration of correlated exchange for neighboring protons is a sufficient criterion for distinguishing exchange via an EX_1 mechanism from EX_2 exchange. Therefore, investigations on the cooperativity of proton exchange have a pivotal role in the present investigation. It must be added that while correlated exchange is a sufficient condition for identification of EX_1 exchange, it is not a necessary condition, since even in an EX_1 regime local protein fluctuations might expose different individual protons in an uncorrelated manner.

To illustrate the use of NOE experiments for distinguishing between correlated and uncorrelated NH exchange (Wagner, 1980), we consider a pair of protons located at a short distance in the protein structure, e.g., two amide protons in an antiparallel β-bridge (Figure 1) or in sequentially adjacent residues

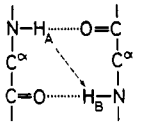

FIGURE 1: Schematic representation of a β-bridge in a regular, antiparallel β-sheet with the two amide protons H_A and H_B on opposite strands at a distance of ca. 2.6 Å (broken arrow).

of an α-helix. If proton A (Figure 1) is selectively saturated, magnetization is transferred to proton B through dipole–dipole interactions. The NOE, η_{AB}, is defined as the ratio of the magnetization change, ΔM_B, to the equilibrium magnetization, M_B^0:

$$\eta_{AB} = \Delta M_B / M_B^0 \qquad (5)$$

η_{AB} depends on the inverse sixth power of the interproton distance and on the overall rotational tumbling and internal mobility of the protein. The influence due to other nearby protons can be reduced to a minimum by selecting sufficiently short buildup periods for the NOE's (Wagner & Wüthrich, 1979b; Anil Kumar et al., 1981).

In a partially deuterated sample, only molecules in which both positions , A and B in Figure 1, are protonated contribute to the NOE, and the magnetization transfer, ΔM_B^{ex}, is reduced relative to the magnetization transfer in a fully protonated reference sample, ΔM_B^{ref}, by the probability of residual protonation for both sites in the same molecule, p_{AB}:

$$\Delta M_B^{ex} = p_{AB} \Delta M_B^{ref} \qquad (6)$$

The NOE observed in a partially exchanged protein preparation then becomes

$$\eta_{AB}^{ex} = \frac{\Delta M_B^{ex}}{M_B^{ex}} = \frac{p_{AB} \Delta M_B^{ref}}{p_B M_B^{ref}} = \frac{p_{AB}}{p_B} \eta_{AB}^{ref} \qquad (7)$$

where p_A and p_B are the probabilities for independent protonation of sites A and B (Figure 1). p_A and p_B can be determined simply by comparing the intensities of the resonances A and B in the ^1H NMR spectra of the partially deuterated protein with those for nonlabile protons. In NOESY spectra, p_A and p_B can also be obtained from measurements of the intensites of cross-peaks manifesting NOE's between the labile protons and nonlabile protons in the partially deuterated protein. In practice, we expect to encounter the following three situations:

(*i*) *Uncorrelated Exchange.* If H_A and H_B are exchanged independently, we have

$$p_{AB} = p_A p_B \qquad (8)$$

and eq 7 reduces to

$$\eta_{AB}^{ex} = p_A \eta_{AB}^{ref} \qquad (9)$$

The NOE is reduced by the factor p_A, which describes the residual protonation of site A.

(*ii*) *Correlated Exchange.* If H_A and H_B can only be exchanged simultaneously, both positions are either protonated or deuterated. Therefore

$$p_{AB} = p_A = p_B \qquad (10)$$

$$\eta_{AB}^{ex} = \eta_{AB}^{ref} \qquad (11)$$

(*iii*) *Contributions from both Correlated and Uncorrelated Exchange.* If we consider H_A and H_B exchange by contributions from both correlated and uncorrelated exchange then

$$\eta_{AB}^{ex} = X \eta_{AB}^{ref} + (1 - X) p_A \eta_{AB}^{ref} \qquad (12)$$

X is the degree of correlation, which describes the relative contribution from the correlated exchange processes:

$$X = (\eta_{AB}^{ex}/\eta_{AB}^{ref} - p_A)/(1 - p_A) \quad (13)$$

For completely correlated exchange, $X = 1$, and we have the limiting situation i. For completely uncorrelated exchange, $X = 0$, corresponding to situation ii.

Materials and Methods

BPTI (Trasylol) obtained from Bayer AG in Leverkusen, West Germany, was used without further purification. Two derivatives of BPTI with reduced thermal stability were used. TRAM-BPTI was prepared by transamination of the N-terminus according to the method of Dixon & Fields (1972) as described in Brown et al. (1978). The characterization of TRAM-BPTI with ^{1}H NMR and ^{13}C NMR by Brown et al. (1978) and Stassinopoulou et al. (1984) showed that after transamination the tertiary structure of BPTI was preserved, with the exception of the N-terminal region, where the modification inhibits the formation of a salt bridge between the C-terminus and the N-terminus.

For the ^{1}H NMR measurements of the NH exchange kinetics, 5–10 mM protein solutions were prepared by dissolving the lyophilized protein in buffered ^2H_2O. Depending on the p^{2}H region studied, 0.1 M phosphate buffer or 0.2 M glycine-d_5 was used. The BPTI solutions further contained 0.3 M NaCl. For a comparative study of BPTI and TRAM-BPTI, 3 M Gdn·HCl was added to the protein solutions. Before the NMR experiments, an approximate adjustment of the p^{2}H was achieved by adjusting the buffer solution without protein. Accurate p^{2}H values were obtained after the NMR experiments were completed by heating the solutions again to the temperatures at which the exchange was investigated (see below) and repeating the p^{2}H measurement with a combination glass electrode at this temperature.

Most of the measurements reported in this paper were obtained at high p^{2}H and elevated temperatures. In contrast to previously reported studies of BPTI [e.g., see Richarz et al. (1979)], the amide proton exchange was then so rapid that the NMR measurements could not be performed at the same conditions as those used for the exchange. Therefore, the following, simple quench procedure was used: 0.4 mL of a freshly prepared ^2H_2O solution of the protein was transferred to an NMR tube. This sample tube was then placed in a thermostat at the temperature where the exchange was to be measured, for example, at 70 °C. After a predetermined time span, the sample was rapidly cooled in ice–water. Subsequently, the ^{1}H NMR spectrum was recorded at 25 °C. This temperature provides a favorable compromise for good spectral resolution and negligible exchange of interior protons during the time needed to record a one-dimensional spectrum. The same protein solution was subjected to 5–10 subsequent exchange cycles, choosing suitable exchange intervals. The residual intensity of fully resolved NH resonances was determined with an accuracy of ca. 5% by simulating the spectra on the Aspect 2000 computer, using Lorentzian line shapes. The areas were normalized relative to the two-proton resonance of the nonlabile C$^\epsilon$ protons of Tyr-23 (Wagner & Wüthrich, 1982a). The kinetics were exponential within experimental error for all resolved NH resonances. Exchange rates for individual amide protons were calculated by exponential regression. With this simple procedure, reliable measurements of rates up to ca. 3 min^{-1} were possible, since the time required to equilibrate the sample in the thermostat, as measured with a fast-response thermocouple, was about 5 s. For some additional measurements of exchange rates which exceeded this limit, a flow apparatus was used which is described in the following paper (Roder et al., 1985).

^{1}H NMR spectra were recorded on Bruker HX 360 and WM 500 spectrometers, which are equipped with Aspect 2000 computers.

For studies of the cooperativity of the exchange in the central β-sheet region of BPTI, one-dimensional truncated-driven NOE difference spectra (Richarz & Wüthrich, 1978; Wagner & Wüthrich, 1979) were recorded with the following pulse sequence: [$-\tau_1(\omega_A)$–90° observation pulse–RD–τ_1-(ω_{off})–90° observation pulse–RD–]. The proton resonance A at frequency ω_A was selectively saturated during the time τ_1, which was immediately followed by the nonselective observation pulse. After a relaxation delay (RD), during which the system was allowed to regain equilibrium, a reference spectrum was recorded with off-resonance irradiation in an empty region of the spectrum at a frequency ω_{off}. The free induction decays obtained with irradiation at ω_A and off-resonance, respectively, were accumulated in different memory locations. They were then subtracted and NOE difference spectra were obtained by Fourier transformation of the difference free induction decay. A value of 0.3 s was chosen for τ_1, which is sufficiently short to avoid falsification of the NOE data for BPTI by spin diffusion (Dubs et al., 1979). The delay time, RD, was 1.0 s. For the NOE experiments with native BPTI, protein concentrations of 20–30 mM were used, and 4000 scans were accumulated for each measurement. For TRAM-BPTI, the concentration was 10–15 mM, and between 8000 and 12000 scans were added up. For the experiments with partially deuterated protein, the samples were exchanged to between 50% and 25% of the initial resonance intensity for the slowly exchanging amide protons. For improved ease of comparison, the NOE measurements for all experiments were obtained under identical conditions. For example, to investigate the cooperativity of the proton exchange at p^{2}H 8.5 and 68 °C, the partial exchange of the protein was obtained by exposing the sample to these conditions for a short time span. The exchange was then stopped by rapid cooling in ice–water, and subsequently the p^{2}H was adjusted to 4.5 by addition of ^{2}HCl. NOE spectra of this solution were then recorded at 25 °C. For the experiments where the exchange was studied in 3M Gdn·HCl, the Gdn·HCl was removed by ultrafiltration before the NOE measurements. To further ensure that the instrumental conditions were unchanged between different experiments, it was verified that corresponding NOE's between amide protons and nearby nonlabile protons, for example C$^\alpha$ protons, were quantitatively identical in the different experiments when measured relative to the residual amide proton resonance intensities in the partially exchanged protein.

Some results on exchange kinetics and cooperativity are also reported for the amide protons in the α-helix and the 3_{10}-helix of BPTI (Deisenhofer & Steigemann, 1975; Kabsch & Sander, 1983). Since these resonances are in a crowded region of the ^{1}H NMR spectrum, they could only be resolved in two-dimensional NMR spectra. Exchange rates were measured with COSY experiments, as described elsewhere in detail (Wagner & Wüthrich, 1982b; Wüthrich & Wagner, 1982). Comparison of the NOE's in the fully protonated and the partially deuterated protein was achieved by analysis of cross sections parallel to ω_1 in NOESY spectra recorded with a mixing time of 0.1 s (Anil Kumar et al., 1981). The procedures used for internal calibration of the relative peak intensities in the NOESY spectra of the fully protonated and partially deuterated protein are described under Results.

Results

p^{2}H Dependence of Exchange Rates. The pH dependence of the NH exchange rates in the range from 4 to 12 was

Table I: Activation Enthalpies for Exchange of Some Interior Amide Protons in BPTI

	$\Delta H^{\ddagger}$ (kcal M^{-1})						
p^2H, temp (°C)	Arg-20	Tyr-21	Phe-22	Tyr-23	Gln-31	Phe-45	kinetic mechanism
8.0, 73–88[a]	79	81	81	81	77	69	EX_1
7.7, 50–70[b]	48	65	65	57	≤30		EX_2–EX_1
8.0, 22–60[c]	29	40	38	42	20	34	EX_2
10.9, 69–81[a]		77	81	73	55		
3.5, 68–80[d]	89	84	88	88	87	81	EX_2

[a] Data from this work (0.3 M NaCl, 0.1 M $Na^2H_2PO_4$). [b] Data from Hilton & Woodward (1979) (0.3 M KCl). [c] Data from Richarz et al. (1979) (no salt). [d] Data from G. Wagner et al. (unpublished results) (no salt).

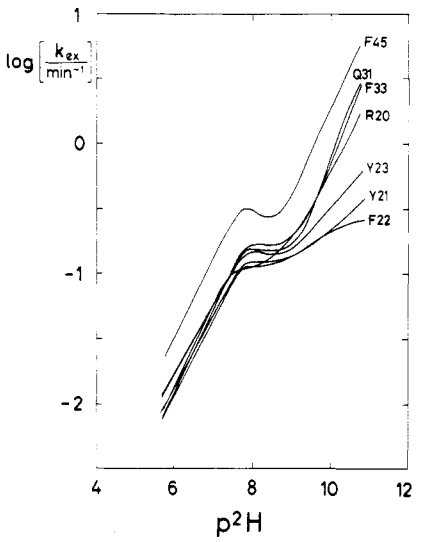

FIGURE 2: Logarithmic plots of the exchange rates vs. p^2H for seven slowly exchanging amide protons of BPTI at 68 °C in ^2H_2O containing 0.3 M NaCl and 0.1 M $Na^2H_2PO_4$ or 0.2 M glycine-d_5, depending on the p^2H.

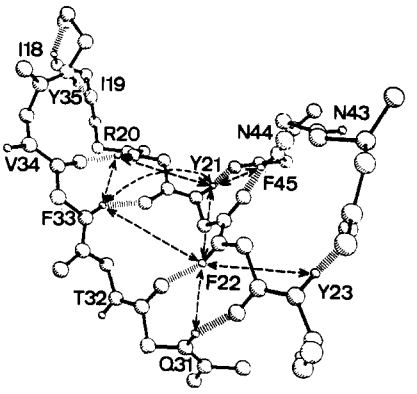

FIGURE 3: Computer drawing of the central part of the antiparallel β-pleated sheet in BPTI (Deisenhofer & Steigemann, 1975). Only the backbone atoms with NH's and carbonyl oxygens, but without $C^{\alpha}H$'s, are shown. The eight NH pairs studied in the NOE experiments are indicated by arrows.

studied for native BPTI at 68 °C in ^2H_2O, 0.3 M NaCl, and 0.1 M $Na^2H_2PO_4$ or 0.2 M glycine-d_5. Figure 2 presents logarithmic plots of the exchange rates vs. p^2H for those seven of the eight most slowly exchanging β-sheet amide protons in BPTI (Wagner & Wüthrich, 1982b) which have well-resolved lines in the one-dimensional ^1H NMR spectra, i.e., Arg-20, Tyr-21, Phe-22, Tyr-23, Glu-31, Phe-33, and Phe-45 (Wüthrich & Wagner, 1979). The locations of these protons in the antiparallel β-sheet are shown in Figure 3. The following qualitative features are readily apparent: For all seven protons, the exchange rate increases linearly with p^2H in the range from p^2H 5.0 to ca. 7.5. From p^2H 7.5 to ca. 9.0, there is a "plateau" where k_{ex} is nearly independent of p^2H. At p^2H above ca. 9.0, the exchange rates increase again with p^2H up to the highest values studied, which are near p^2H 12.0. For Phe-22, there is an indication that the plot of log k_{ex} vs. p^2H might level off again at p^2H above ca. 10.5. It can further be seen that closely similar exchange rates for six of these seven protons prevail in the p^2H range just below the plateau region and that there is a marked dispersion of the exchange rates in the region of strong p^2H dependence which follows the plateau. It should be added that all p^2H measurements were made at the exchange temperature of 68 °C, as described under Materials and Methods.

Additional measurements of the p^2H dependence of k_{ex} for the same seven amide protons were obtained for both BPTI and TRAM-BPTI at 55 °C in 3 M Gdn·HCl and 0.05 M NaH_2PO_4. In Figure 4, logarithmic plots of the p^2H dependence of k_{ex} in all three samples studied are superimposed. In all cases, the qualitative behavior is similar to that described above for BPTI at 68 °C. A nearly p^2H-independent plateau sets in between p^2H 7 and 8. Above p^2H 9 for BPTI and above p^2H 10 for TRAM-BPTI, the slope of log k_{ex} increases again.

For BPTI and TRAM-BPTI, the p^2H profiles below p^2H 7 were also recorded. They were found to be similar to those observed for the same protons in BPTI under somewhat different conditions (Richarz et al., 1979). The measurements for BPTI at 68 °C represent an extension of the data from Hilton & Woodward (1979) into the high p^2H range.

Temperature Dependence of Exchange Rates. The temperature dependence above 60 °C of the exchange rates for some interior amide protons in a solution of BPTI in 0.3 M NaCl and 0.1 M $Na^2H_2PO_4$ was measured at p^2H 8.0 and at p^2H 10.9. The rates were measured with the quench techniques described under Materials and Methods. The data are presented in Figure 5 in the Arrhenius representation. At p^2H 10.9, only the four most slowly exchanging protons had rates within the experimentally accessible range. Apparent activation enthalpies are listed in Table I. The points at the lowest temperatures studied (not shown in Figure 5) deviated systematically from linear behavior, and they were not included in the linear regression analysis.

NOE Studies of the Cooperativity of Exchange. One-dimensional truncated-driven nuclear Overhauser difference spectroscopy was used to study the cooperativity of exchange among the seven amide protons in the β-sheet of BPTI for which the p^2H dependence of the exchange was measured (Figures 2 and 4). The conclusions obtained relied on observation of NOE's between the eight pairs of protons which are connected by arrows in Figure 3.

Figure 6 presents typical experimental NOE results. The bottom trace of Figure 6A shows the region from 8 to 11 ppm of the ^1H NMR spectrum of a freshly prepared BPTI solution in ^2H_2O, which contains exclusively amide proton resonances (Masson & Wüthrich, 1973). The resonance assignments (Dubs et al., 1979) are also indicated. The upper trace in Figure 6A shows the NOE differenece spectrum obtained in this solution with preirradiation on the amide proton of Phe-22.

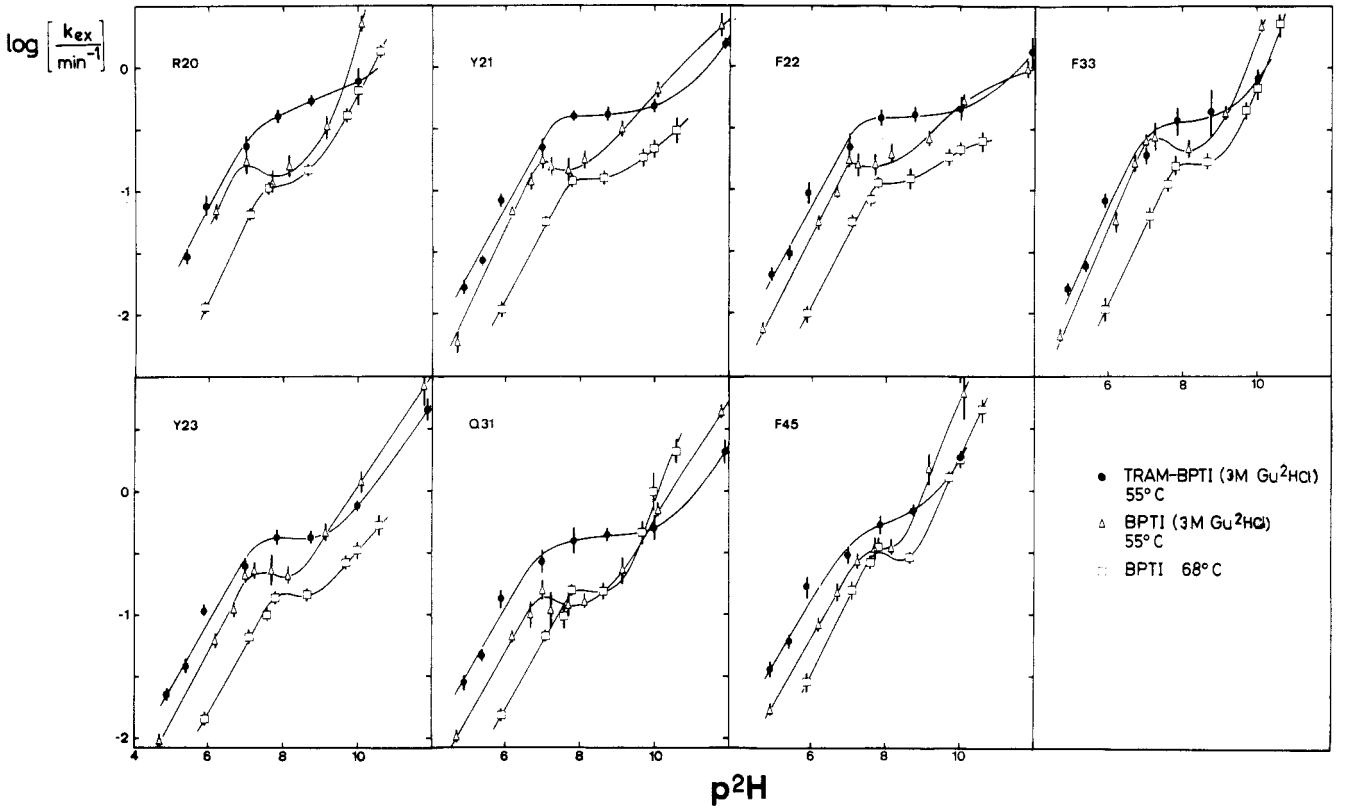

FIGURE 4: Logarithmic plots of the exchange rates as a function of p^2H for seven amide protons in the following systems: (□) BPTI exchanged at 68 °C in ^2H_2O containing 0.3 M NaCl and either 0.1 M $Na^2H_2PO_4$ or 0.2 M glycine-d_5, depending on the p^2H values. (△) BPTI exchanged at 55 °C in ^2H_2O containing 3 M Gdn·HCl. (●) TRAM–BPTI exchanged at 55 °C in ^2H_2O with 3 M Gdn·HCl and 0.05 M $Na^2H_2PO_4$. The vertical error bars indicate the standard deviation of the exponential regression used to calculate the rates. Curves are drawn by hand to guide the eye.

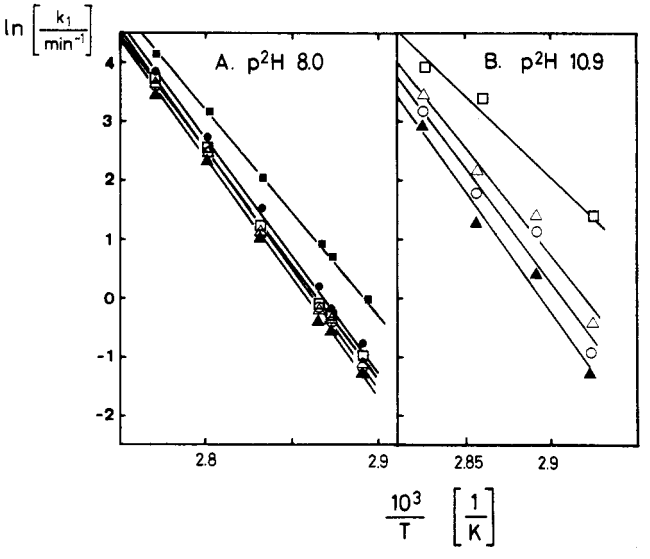

FIGURE 5: Arrhenius plots for selected amide proton exchange rates in BPTI at p^2H 8.0 and 10.9 in ^2H_2O containing 0.3 M NaCl and 0.1 M $Na^2H_2PO_4$: Arg-20 (●); Tyr-21 (○); Phe-22 (▲); Tyr-23 (△); Gln-31 (□); Phe-45 (■). Straight lines were calculated by linear regression using the rates obtained in the range $10^3/T < 2.90$ at p^2H 8.0 and $10^3/T < 2.95$ at p^2H 10.9.

Because of the limited selectivity of the preirradiation, the peaks at the positions of Phe-45 and Tyr-35 are due to direct saturation of these resonances. NOE's due to dipolar coupling with Phe-22 are observed for the amide protons of Tyr-23, Phe-33, Tyr-21, and Gln-31. Inspection of Figure 3 shows that these four amide protons are located nearest to that of Phe-22. Panels B and C of Figure 6 show the corresponding results obtained after ca. 50% of the amide protons were exchanged with ^2H at 68 °C and p^2H 6.0 or p^2H 8.0, respectively. After the exchange at p^2H 6.0 (Figure 6B), the NOE's on Tyr-23, Phe-33, Tyr-21, and Gln-31 had ca. 50% of the intensity observed before exchange, when the NOE's were calibrated against the intensities of the preirradiated line of Phe-22 in the two experiments. After the exchange at p^2H 8.0 (Figure 6C), NOE's essentially identical with those in Figure 6A were obtained. Following eq 9 and 11, we conclude that the exchange in the central β-sheet of BPTI is correlated at p^2H 8.0 and 68 °C and uncorrelated at p^2H 6.0 and 68 °C.

Experiments of the type of Figure 7 were carried out with preirradiation on each of the amide protons of residues 20–23, 31, 33, and 45 (Figure 3). For each pair of protons connected by an arrow, the average of the NOE's obtained with preirradiation on either proton was obtained. From these data, the degree of correlation, X, was then computed with eq 13. Figure 7 presents the p^2H dependence of X for BPTI in ^2H_2O solution at 45 and 68 °C. Figure 8 contains the corresponding data for BPTI in 3 M Gdn·HCl at 55 °C. The error bars in Figures 7 and 8 indicate the statistical errors estimated from the uncertainty of the intensity determination. The strong NOE's for the pairs Phe-22/Gln-31, Arg-20/Phe-33, and Tyr-21/Phe-45, which are all between residues in an antiparallel β-bridge (Figure 3), lead to the most reliable data. For the other pairs, the errors are bigger because of the intrinsically weaker NOE's due to the larger distance between the protons, and in some cases also because of the small separation of the resonances in the ^1H NMR spectrum (Figure 6), which limits the selectivity of irradiation. Figure 7 shows that for BPTI exchanged at 45 °C less than 20% contribution from correlated exchange was found between p^2H 6 and 10. Combined with the linear increase of log k_{ex} with p^2H observed by Richarz et al. (1979), this strongly indicates that under

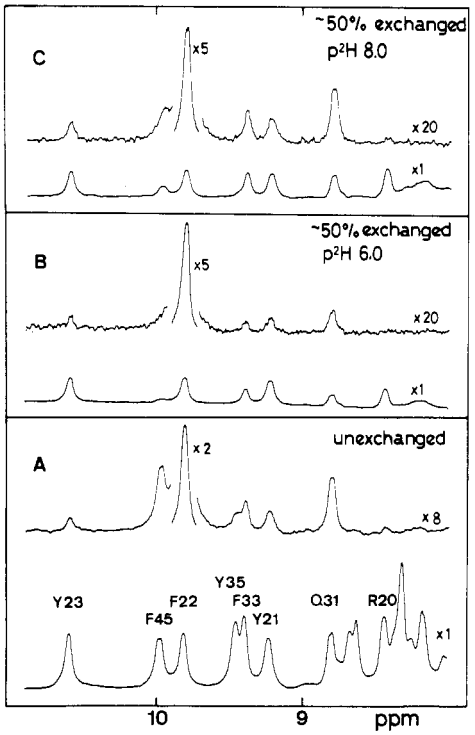

FIGURE 6: Truncated-driven NOE experiments in partially exchanged BPTI. The top trace in each panel shows the NH region of the NOE difference spectrum obtained by irradiating the NH resonance of Phe-22, and the lower trace shows the corresponding unperturbed spectrum. Spectra were recorded at 24 °C, p²H 4.5. For a better presentation, the NOE difference spectra and the resonances of the irradiated protons were expanded vertically by the factors indicated in the figure. For reference, panel A shows the NOE spectrum of a fully protonated BPTI sample. Before the spectra in panels B and C were recorded, the samples were exchanged to ca. 50% of the NH intensity at 68 °C, p²H 6.0 (B) and p²H 8.0 (C), respectively.

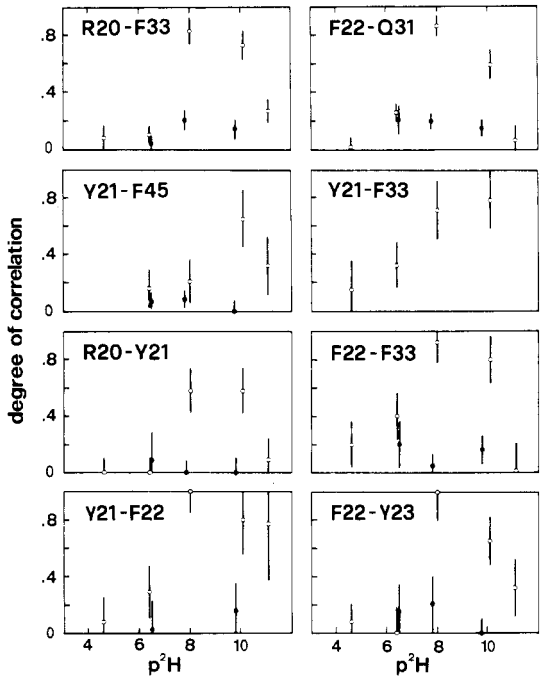

FIGURE 7: Plots of the degree of correlation, X, calculated with eq 13 as a function of p²H for eight pairs of amide protons in BPTI after partial exchange at 68 (○) and 45 °C (●). The vertical bars indicate estimates of the error limits (see text).

these conditions the exchange is dominated by an EX$_2$ process, which is intrinsically uncorrelated. In BPTI exchanged at 68 °C, the degree of correlation increased for most NH pairs from

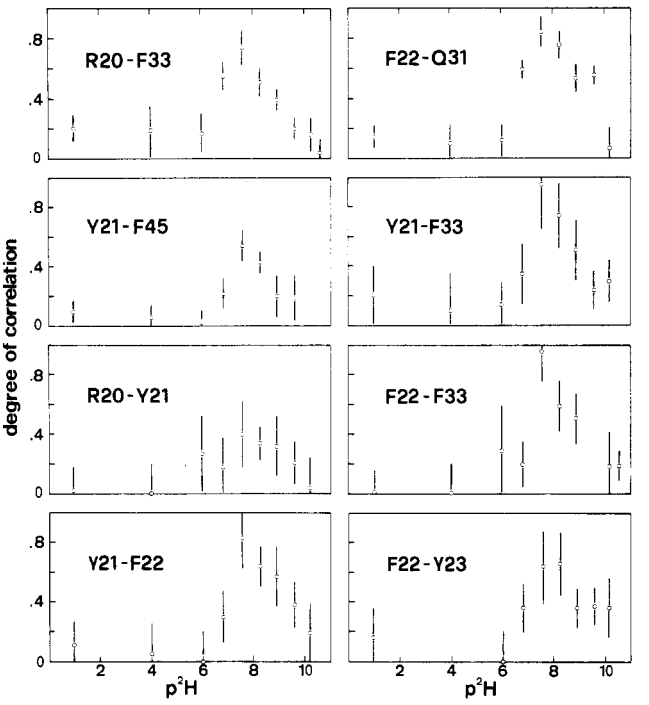

FIGURE 8: Degree of correlation as in Figure 8 for BPTI after partial exchange in ^2H_2O and 3 M deuterated Gdn·HCl at 55 °C.

values below 0.2 to peak values near 1 between p²H 6 and 8. At p²H above 8, the degree of correlation decreased again. Very similar behavior, with a pronounced peak in the degree of correlation near p²H 8.0, was observed for BPTI which was dissolved in 3 M Gdn·HCl and partially exchanged at 55 °C (Figure 8).

To further investigate whether the unusual p²H dependence of the exchange rates and the correlated exchange around p²H 8.0 could be connected with the deprotonation of the N-terminal amino group, which has a pK_a value of 8.0 (Brown et al., 1978), NOE studies were also performed with TRAM-BPTI. For direct comparison with BPTI, partial exchange was achieved in 3 M Gdn·HCl at 55 °C. Results closely similar to those with BPTI were obtained. The transition from a low to a high degree of correlation occurred near p²H 7.0. The regime of correlated exchange was found to be somewhat broader than for BPTI and to extend up to ca. p²H 10.

Additional NOE measurements of the cooperativity of exchange were done for the amide protons in the α-helix from residues 47–54 and the 3_{10}-helix from residues 5–7 in BPTI (Deisenhofer & Steigemann, 1975; Kabsch & Sander, 1983). Compared to the central β-sheet, the exchange in the helical segments is considerably faster and was therefore only accessible to the NMR measurements when milder conditions of p²H and temperature were used. Furthermore, the resonance lines for most of the helical amide protons are not sufficiently well resolved to be studied quantitatively with one-dimensional experiments. For these reasons, experiments of the type illustrated in Figure 9 were used.

Figure 9 shows a region of a NOESY spectrum of a freshly dissolved solution of BPTI in ^2H_2O, p²H 3.5, which contains NOE cross-peaks with amide protons. Figure 10A shows a cross section along ω_1 at the ω_2-position of the amide proton of Met-52, which is located in the middle of the α-helix. This position is indicated in Figure 9 with an arrow and a broken line parallel to the ω_1 axis. In Figure 10A, the position of the diagonal amide proton line of Met-52 is indicated with a star. Three NOE cross-peaks to other amide protons are identified in Figure 10A, and some NOE's to nonlabile protons are

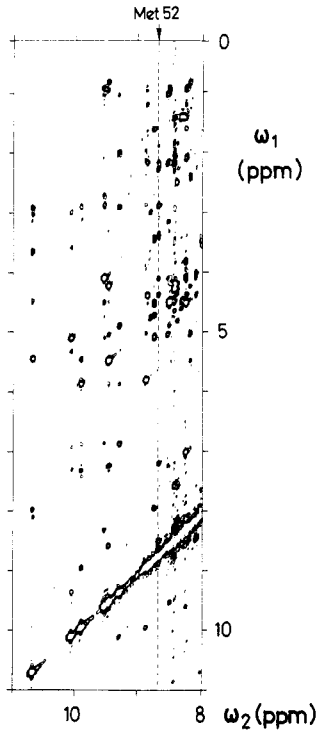

FIGURE 9: Low-field region of a 500-MHz NOESY spectrum of a 10 mM solution of BPTI recorded at p^{2}H 3.5, 24 °C, just after the protein was dissolved in ^2H_2O. The mixing time was 100 ms. The position of the cross section used for Figure 10 is indicated with an arrow and a broken line.

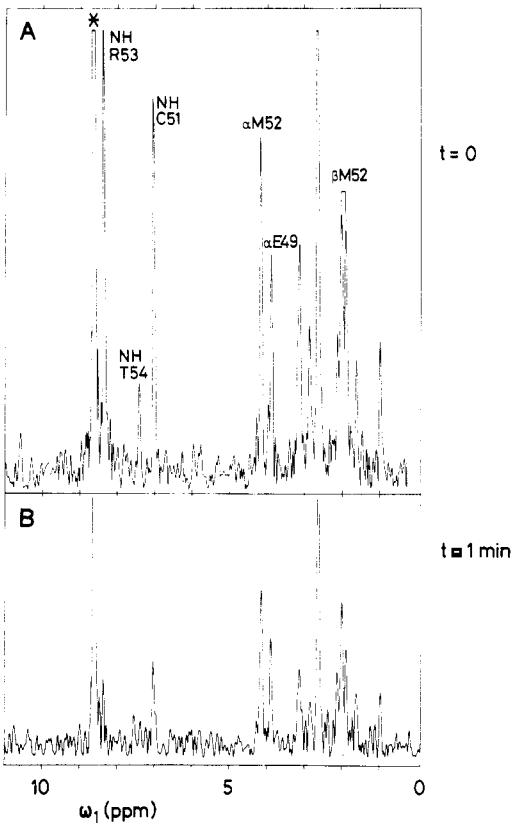

FIGURE 10: Cross sections from 500-MHz NOESY spectra of BPTI taken parallel to the ω_1 axis at the ω_2-position of the amide proton of Met-52. (A) Recorded in a freshly prepared ^2H_2O solution; (B) recorded at p^{2}H 3.5, 24 °C, after the sample had been kept for 1 min at 46 °C and p^{2}H 8.0. The partial exchange can be recognized from the decrease of the NOE cross-peaks to nonexchangeable protons. The degree of correlation can be obtained from cross-peaks to other labile protons. Some cross-peaks are identified in (A).

identified in the spectral region from ω_1 = 0–5 ppm in Figure 10A. A corresponding NOESY spectrum (Figure 10B) was recorded in a BPTI solution which had been partially exchanged by exposure for 1 min to 45 °C and p^{2}H 8.0 and then rapidly cooled and acidified to p^{2}H 3.5 by addition of ^{2}HCl. During 1 min at 45 °C and p^{2}H 8.0, the amide protons of the α-helix were exchanged to a residual protonation of 20–50% (Richarz et al., 1979). The NOESY spectrum was recorded with the same number of scans, and the same vertical expansion as in Figure 10A was used for the cross section in Figure 10B. Thus, the degree of protonation, $p_{\text{Met-52}} \approx 0.45$, could be obtained from the intensity ratios of the NOE cross-peaks to nonlabile protons in the two cross sections of Figure 10A,B. The probability for simultaneous protonation, p_{AB}, of two adjacent peptide groups can be obtained from the intensity ratios of the NOE cross-peaks between the amide protons. Thus, we found that $p_{\text{Met-52,Cys-51}} \approx 0.22$ and $p_{\text{Met-52,Arg-53}} \approx 0.15$. This shows that $p_{AB} = p_A p_B$, which indicates uncorrelated exchange at these conditions of temperature and p^{2}H. The same observation was made for all other amide protons of the α-helix and for all protons of the 3_{10}-helix.

A further NOESY experiment was carried out with a sample which had been kept for 2 min at 80 °C and p^{2}H 3.5, whereby the amide protons of the β-sheet were exchanged to about 50%. A comparison of the intensities of the NOE cross-peaks between the amide protons of Phe-22 and Glu-31, Ile-18 and Tyr-35, and Arg-20 and Phe-33 showed that the hydrogen–deuterium exchange was uncorrelated in the β-sheet under these experimental conditions.

Discussion

Considering the fundamental features of cooperative proton exchange expressed by eq 1–12, we arrive at the following qualitative conclusions on the exchange mechanisms which prevail for different individual amide protons in BPTI solutions at different conditions of p^{2}H and temperature. In the p^{2}H region from 1 to ca. 7.0, the data available (Richarz et al., 1979; Hilton & Woodward, 1978; Figures 2, 4, 7, and 8) indicate that the exchange is by an EX_2 mechanism at all experimentally accessible temperatures. At p^{2}H values from ca. 7 to 9 and at temperatures above ca. 55 °C, exchange by an EX_1 process becomes dominant. A plateau in the plots of log k_{ex} vs. p^{2}H (Figures 2 and 4) is reached in this p^{2}H range, since the efficiency of the EX_1 exchange mechanism changes little with further increase of p^{2}H above 7. [While EX_1 exchange appears to be common in nucleic acids (Englander & Kallenbach, 1984), we are not aware of previous experimental verifications of EX_1 exchange in proteins. In a broad discussion on the p^{2}H dependence of amide proton exchange in BPTI, Hilton & Woodward (1979) did, however, invoke the possibility that EX_1 exchange might also affect the experimental observations.] However, at p^{2}H above ca. 9, the rates increase again with p^{2}H (Figure 2). Simultaneously, the rates become different for the individual protons, and the exchange is predominantly uncorrelated again (Figures 7 and 8). This indicates that local, noncooperative structure fluctuations play a dominant role for hydrogen exchange in this p^{2}H range. Woodward & Hilton (1980) have discussed this phenomenon on the basis of a two-process model which is in several aspects consistent with our interpretation as discussed below. In the following, we evaluate the parameters which govern the exchange in the different regimes and investigate possible structural interpretations of the exchange kinetics.

Kinetic Parameters Governing EX_1 Exchange in BPTI. Exchange via EX_1 process is directly related to the opening

Table II: Representative Parameters Derived from NH Exchange in BPTI and TRAM-BPTI in the EX_2 Limit, in the EX_1 Limit, and at Basic p^2H

protein, temp (°C)	amino acid residue	p^2H_{tr}[a]	k_2^g (min^{-1})[b]	k_1^g (min^{-1}) at p^2H 8.6[c]	k_{ex} (min^{-1}) at p^2H 10.6[d]
BPTI, 68, ^2H_2O	R20	7.8	1.2×10^5	0.15	1.4
	Y21	7.8	1.5×10^5	0.13	0.31
	F22	7.8	9.4×10^4	0.12	0.25
	Y23	7.9	1.2×10^5	0.14	0.53
	Q31	7.8	2.6×10^5	0.15	2.1
	F33	7.9	1.9×10^5	0.17	2.2
	F45	7.7	1.7×10^5	0.29	4.4
BPTI, 55, 3 M Gdn·HCl	R20	7.3	1.6×10^4	0.12	2.3
	Y21	7.4	2.5×10^4	0.15	0.66
	F22	7.4	1.6×10^4	0.16	0.53
	Y23	7.3	1.2×10^4	0.23	1.2
	Q31	7.0	1.8×10^4	0.12	0.71
	F33	7.3	2.0×10^4	0.24	2.2
	F45	7.4	3.5×10^4	0.34	6.0
TRAM-BPTI, 55, 3 M Gdn·HCl	R20	6.9	6.2×10^3	0.40	10
	Y21	6.9	7.9×10^3	0.41	1.6
	F22	7.0	6.2×10^3	0.39	1.3
	Y23	7.1	7.9×10^3	0.43	4.6
	Q31	6.9	1.4×10^4	0.40	2.1
	F33	7.0	9.9×10^3	0.37	10
	F45	7.5	4.4×10^4	0.53	10

[a] p^2H of transition from EX_2 to EX_1 mechanism at $k_2 = k_3$ as determined from Figure 4. [b] k_2^g, the closing rate for global fluctuations, was obtained from the transition from EX_2 to EX_1 exchange with $k_2^g = k_3$, which is the onset of the p^2H-independent exchange "plateau" in Figures 2 and 4. [c] k_1^g is the opening rate for global fluctuations. It was obtained from the exchange rate in the plateau region at p^2H 8.6 for BPTI at 68 °C, at p^2H 7.7 for BPTI in 3 M Gdn·HCl, and at p^2H 7.9 for TRAM-BPTI in 3 M Gdn·HCl. [d] At basic p^2H, the kinetic mechanism is still ambiguous, and only the experimental exchange rate, k_{ex}, is given.

rate, k_1 (eq 3), which can thus be evaluated from the data in the plateau regions above p^2H 7 (Figures 2 and 4). Table II shows that in the different systems studied, k_1 is between 0.12 and 0.53 min^{-1} at p^2H 8.6. The closing rate, k_2 (eq 1), can also be obtained by using $k_2 = k_3$ at the p^2H value where the EX_2 process changes to an EX_1 process. The values for k_2^g in Table II were thus evaluated on the basis of k_3 values computed with the rules of Molday et al. (1972) and activation enthalpies given by Englander & Poulsen (1969). The temperature dependence of the water dissociation constant was estimated after Covington et al. (1966) as described by Roder et al. (1985). The resulting k_2 values in the three systems studied cover the range from 6×10^3 to 2.6×10^5 min^{-1} (Table II).

Since individual resonance assignments are available for BPTI (Wagner & Wüthrich, 1982a) and TRAM-BPTI (Stassinopoulou et al., 1984), these fluctuation rates can be attributed to precisely defined locations in the amino acid sequence and the spatial structure (Deisenhofer & Steigemann, 1975). In BPTI at 68 °C, the residues in the central part of the β-sheet, Arg-20, Tyr-21, Phe-22, Tyr-23, Gln-31, and Phe-33 (Figure 3), have strikingly similar rates, k_1, extending over the narrow range from 0.12 to 0.17 min^{-1}. This is consistent with the observation that the exchange in the central β-sheet is correlated in the plateau region (Figures 7 and 8), and we conclude that these amide protons are exposed to the solvent by a cooperative opening of the whole β-sheet. The amide protons of the more peripheral β-sheet residues Ile-18, Tyr-35, and Phe-45 have considerably faster exchange rates (Richarz et al., 1979), which implies that additional, more strictly localized structure fluctuations contribute significantly to the exchange of these protons.

Limitations on Studies of EX_1 Exchange in Proteins. EX_1 exchange provides very direct access to the kinetic parameters needed for characterization of protein structure fluctuations. However, in BPTI, the EX_1 exchange prevails only over a narrow range of experimental conditions, i.e., at p^2H 7–9 and temperatures above 55 °C. More generally, the parameters in Table II imply that EX_1 exchange in proteins should only rarely be measurable with the presently available techniques. This can readily be rationalized, because the intrinsic exchange rates, k_3, are slow compared to the closing rates, k_2 (Table II), except possibly at high temperature and high p^2H. When such extreme conditions are approached, the amide proton exchange rates in most globular proteins become too fast to be measured by NMR, or the proteins even denature before EX_1 conditions are attained. An illustrative example is provided by the exchange in the α-helix of BPTI (Figures 9 and 10). Under the conditions where EX_1 exchange prevails for the central β-sheet in the same protein (Figures 2 and 7), the exchange in the helix is too rapid to be measured. Conversely, with all conditions which enable quantitative exchange measurements for the α-helix, uncorrelated exchange was observed (Figure 10).

Structural Interpretation of EX_2 Exchange. In contrast to EX_1 exchange, EX_2 exchange can for fundamental reasons (eq 4) not be directly related to the kinetics of protein structure fluctuations, and no unambiguous conclusions on the cooperativity of the exchange can be drawn from NH exchange studies in this regime. However, there are additional observations among the data collected for BPTI which indicate that in the p^2H range below p^2H 7 (Figures 2 and 4) the EX_2 exchange in the central part of the β-sheet is propagated by global fluctuations of this secondary structure element. The strongest inference comes from the observation in the EX_1 regime between p^2H 7 and 9 (Figures 2 and 4) that exchange for these amide protons is propagated by concerted fluctuations in the β-sheet. That the same type of internal mobility persists at lower p^2H is compatible with the small dispersion of the overall exchange rates for the amide protons of Arg-20, Tyr-21, Phe-22, Tyr-23, Gln-31, and Phe-33 in the p^2H range 5–7 (Figure 2) and with the data on the equilibria k_1/k_2 [eq 4; see below and Wagner et al. (1984)]. We therefore refer to the closing rate, k_2, in the transition region from EX_2 to EX_1 exchange near p^2H 7.0 as the closing rate for "global" fluctuations in the β-sheet, k_2^g (Table II).

For the practical purpose of studying protein internal motility with the use of amide proton exchange measurements, the most important conclusion from the present investigation is that such projects will usually have to rely on data from EX_2 exchange. It is therefore of imminent interest that while EX_2 exchange rates for amide protons cannot be directly correlated with the kinetics of intramolecular motions, EX_2 data combined with individual ^1H NMR assignments for the protons studied can be used to investigate the relative populations of closed and open states, N and O (eq 1), in a dynamic protein structure. Since this was recently discussed elsewhere in detail (Wagner, 1983; Wagner et al., 1984; Englander & Kallenbach, 1984), only a brief summary is included here.

The structural analysis of EX_2 exchange data relies on eq 4. Once sequence-specific resonance assignments for the amide protons have been obtained (Wagner & Wüthrich, 1982a), the intrinsic exchange rates, k_3, corresponding to the measured overall rates, k_{ex}, can be computed with the rules of Molday et al. (1972) [see also Roder et al. (1985)]. With eq 4, the equilibrium constant $K = k_1/k_2$ can then be evaluated. In logarithmic plots of k_{ex} vs. k_3

$$\log k_{ex} = \log k_3 + \log (k_1/k_2) \quad (14)$$

the data points for all those amide protons for which exchange is promoted by structure fluctuations with identical populations of the open states (eq 1) will lie on a straight line with slope 1. The intercepts of these lines with the log k_{ex} axis at log k_3 = 0 give log (k_1/k_2). From studies at variable temperature, the thermodynamic parameters governing the fluctuations between open and closed states of the protein conformation (eq 1) can then be further evaluated. On the basis of these considerations, it could be demonstrated for BPTI and a chemically modified form of BPTI that the fluctuations which promote the exchange from the central part of the β-sheet (Figure 3) have the same value of k_1/k_2 for all individual amide protons in this region. Different values for k_1/k_2 were found for peripheral locations in the β-sheet, and evidence for multiple fluctuation types promoting exchange within the C-terminal α-helix and within the N-terminal 3_{10}-helix was obtained (Wagner et al., 1984).

Amide Proton Exchange in BPTI at High p²H and High Temperature. While the available data are sufficient for an unambiguous characterization of the mechanisms which govern the exchange in BPTI solutions at p²H values up to ca. 9, the onset of uncorrelated exchange with sizable p²H dependence at p²H values above 9 (Figures 2, 4, 7, and 8) could a priori be caused by different exchange mechanisms. Considering that different exchange rates prevail for the individual amide protons and that the exchange is uncorrelated, local structure fluctuations must play an important role in this p²H range. It would then appear that there are two possible, fundamentally different mechanisms which may cause the transition from global to local exchange when these extreme conditions of temperature and p²H are approached. In the following, we refer to these as the "kinetic switch model" and the "deprotonation switch model". The kinetic switch model invokes that different types of fluctuations are present at all experimental conditions of p²H and that these are redistributed with temperature due to different enthalpies. Within the framework of this model, hydrogen exchange measurements at extreme conditions of temperature and p²H would provide interesting insights into protein fluctuations which are at different conditions masked by rare, but more efficient, global fluctuations. In contrast, the deprotonation switch model invokes fluctuations which are present only at high p²H. Following this model, the hydrogen exchange measurements at high p²H and high temperature would mainly provide an insight into the protein behavior on its way toward alkaline denaturation.

In the kinetic switch model, we assume that there are two classes of internal motions, which we call "global" and "local" with the kinetic parameters k_1^g and k_1^l, respectively. The global and local structure fluctuations must have sizably different closing rates, k_2, and different populations of open states, k_1/k_2, as follows. k_2^l must be much larger than k_2^g so that the transition from EX_2 to EX_1 exchange (at $k_2 = k_3$) occurs only at higher p²H for the local fluctuations. The equilibrium for the global fluctuations must be more strongly shifted to the open states, O, with $k_1^g/k_2^g > k_1^l/k_2^l$, so that the global fluctuations are dominant for the exchange as long as EX_2 exchange prevails for both the global and the local fluctuations. Note that this condition could be attained entirely as a consequence of k_2^l being large compared to k_2^g and that local openings might indeed be expected to close faster than global openings. With this model, the observed p²H profiles (Figures 2 and 4) and the loss of correlated exchange at high p²H (Figures 7 and 8) could be explained without any requirements for p²H-dependent changes of the relative populations of the global and local classes of fluctuations. If the exchange rates could be measured to even higher p²H than the data in Figures 2 and 4, the kinetic switch mechanism would predict another plateau for the p²H region where $k_3 \geq k_2^l$. Since this effect is not observed up to p²H 12 (Figure 4), k_2^l must be $\geq k_3$ (68 °C, p²H 12) $\approx 2.5 \times 10^7$ s^{-1}. For this estimate, the intrinsic exchange rate, k_3, was extrapolated from the model peptide data of Englander & Poulsen (1969) and Molday et al. (1972).[2]

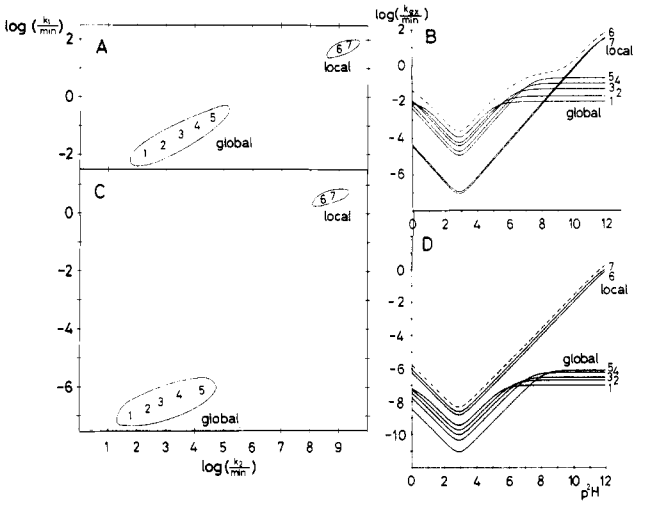

FIGURE 11: p²H and temperature dependence of the exchange of a single amide proton in BPTI resulting from a hypothetical distribution of global and local fluctuations. (A) Distribution of five global and two local fluctuations (characterized by parameters k_1^i and k_2^i; see text) at high temperature (68 °C) in a log k_1 vs. log k_2 plot. (B) Plot of log k_{ex} vs. p²H resulting from the structure fluctuations in (A). Solid lines, contributions from the individual fluctuations; dashed line, overall exchange rate. (C) Same as (A) for low temperature (36 °C). For k_1, a strong temperature dependence and for k_2 a small temperature dependence were assumed. (D) Same as (B) for the low-temperature structure fluctuations shown in (C).

A schematic survey of the manifestations of such a kinetic switch mechanism over the entire p²H range from 1 to 12 is provided by Figure 11. In this figure, we assume, in addition to the features discussed above, that we have two classes of intramolecular motions, global and local, respectively, with each of them containing a multitude of slightly different fluctuations, i, with discrete values of k_1 and k_2. Panels A and C of Figure 11 give hypothetical distributions of k_1^i and k_2^i, in a two-dimensional representation, at high temerature (68 °C) and low temperature (36 °C), respectively. Figure 11B,D shows the corresponding overall exchange rates in a log k_{ex} vs. p²H representation, where k_{ex} is the sum of the contributions from the different fluctuations:

$$k_{ex} = \sum_i \frac{k_1^i k_3}{k_2^i + k_3} \quad (15)$$

[2] The quantitative estimation of k_2 and k_1/k_2 from eq 2 and 4 depends crucially on the assumption that the intrinsic exchange rates, k_3, are identical with those in model peptides and can be extrapolated from the data of Molday et al. (1972) and Englander & Poulsen (1969). One could imagine, however, that for local fluctuations the resulting solvent accessibility of the amide protons is still limited when compared to global fluctuations (or, of course, small model peptides). In the model of eq 1, this might be accounted for by using a smaller apparent "intrinsic" exchange rate, k_3^l, for exchange from local openings. This would make local fluctuations less effective for promoting hydrogen exchange, and it would shift the EX_2 to EX_1 transition to higher p²H. Following these considerations, the present use of the transition condition $k_2 = k_3$ could lead to an overestimation of k_2.

k_1 and k_2 for the individual fluctuations were chosen so that they fit approximatel the experimetnal data at 68 °C in the p^2H range 7–11. For the temperature dependence of the equilibrium constants, k_1^i/k_2^i, the enthalpy, ΔH, was taken to be 70–80 kcal/M for the global fluctuations and ~10 kcal/M for the local fluctuations. It was further assumed that the distribution of the individual k_2^i is almost independent of temperature and that most of the temperature dependence of the equilibrium constant k_1/k_2 goes on account of k_1 (Pohl, 1976; Roder, 1981; Englander & Kallenbach, 1983). We thus have at high temperature that $k_1^g/k_2^g > k_1^l/k_2^l$, whereas at low temperature $k_1^g/k_2^g < k_1^l/k_2^l$ (Figure 11A,C). At high temperature (Figure 11B), only global fluctuations contribute to the hydrogen exchange up to p^2H ~9. The different global fluctuations reach the EX_1 limit at somewhat different p^2H values. As long as there remain some global fluctuations with $k_2^i > k_3$, predominant exchange by an EX_2 mechanism is observed overall. At $p^2H \gtrsim 7$, all global fluctuations provide exchange via the EX_1 mechanism, and thus, overall this mechanism is dominant up to the onset of more efficient exchange by local fluctuations near p^2H 9. In the base-catalyzed regime between p^2H 4 and 7 at high temperature, this picture would predict a slope <1 in the plot of log k_{ex} vs. p^2H (see Figure 11B). At low temperature, local fluctuations would be dominant over the whole p^2H range, and a "normal" p^2H dependence should prevail (Figure 11D). These predictions of the model are consistent with experimental observations [compare, e.g., Hilton & Woodward (1979)].

In the deprotonation switch model, we assume that EX_1 exchange prevails over the entire p^2H range from the onset of the plateau near p^2H 7.5 to p^2H 12. The loss of correlated exchange at $p^2H \gtrsim 9$ would be explained with a transition from global fluctuations to strictly local opening processes, where only single amide groups would be exposed to the solvent. In this model, the local character of the structure fluctuations at $p^2H \gtrsim 9$ would be a consequence of the deprotonation of ionizable groups, which would lead to a loss of intramolecular salt bridges and thus reduce the cooperativity of the fluctuations. Since the onset of uncorrelated exchange lies at $p^2H \gtrsim 9$, the titration of the N-terminus, the four tyrosines, and the four lysines would have to be responsible for this effect in BPTI. The increase of the exchange rates, $k_{ex} = k_1$, with p^2H would be due to increasing destabilization of the protein structure because of the titration of the same ionizable groups between p^2H 9 and 12 (Figure 2).

There are conditions where both exchange mechanisms appear to coexist, albeit in different regions of the molecule. Let us consider the pH, temperature, and correlation data measured in the absence of denaturant (Figures 2, 5, and 7). The amide protons of Tyr-21, Phe-22, and Tyr-23, which are located on the central strand of the β-sheet (Figure 3), have properties compatible with the deprotonation switch model: At both p^2H 8.0 and p^2H 10.9, their activation enthalpies are large (73–81 kcal M^{-1}; Table I); the rate increase toward basic p^2H is comparatively weak (Figure 2); Tyr-21 and Phe-22 exchange at similar rates (Figure 2), and the pairwise correlation at 68 °C remains high up to p^2H 11 (Figure 7). These properties are incompatible with the localized nature of the rapid fluctuations which would be required by the kinetic switch mechanism. With the deprotonation switch model, the rates are interpreted as opening rates, and the increase of k_1 above p^2H 8 reflects the destabilization of the native protein structure by the deprotonation of the basic residues (N-terminus, Tyr and Lys). The high-pH behavior of the remaining amide protons is, however, quite different and shows the characteristics of the kinetic switch mechanism. They are characterized by much stronger pH dependences (up to a factor of 8 rate increase per pH unit), which is indicative of an EX_2 mechanism, and smaller temperature dependences, as seen for Gln-31 in Figure 5B. The rate divergence with increasing pH, associated with decreased correlation, suggests that rapid, localized fluctuations dominate the exchange in all but the most stable regions of the molecule.

Additional insight can be gained by comparison of BPTI with TRAM-BPTI (Figure 4), which affords information on the influence of the deprotonation of the N-terminus on amide proton exchange. The transition from low-p^2H EX_2 exchange to EX_1 exchange is near the pK_a value for the N-terminal amino group in BPTI (Brown et al., 1978). Figure 4 and Table II show that in the measurements recorded at 55 °C and in 3 M Gdn·HCl, the transition is at a slightly lower p^2H for TRAM-BPTI than for BPTI. This indicates that the closing rate, k_2, is slightly decreased (by a factor ≤ 3) by the chemical modification of the N-terminus. Furthermore, the k_{ex} values due to EX_1 exchange in TRAM-BPTI are somewhat higher than in BPTI (Figure 4), indicating that the opening rates, k_1, are slightly higher (by factors of 1.5–3.3) in TRAM-BPTI (Table II). With regard to distinguishing between the two proposed mechanisms for the switch to noncooperative exchange at high p^2H, we note that the kinetic switch model would provide a straightforward explanation of the experimental data for TRAM-BPTI. Since k_1 is faster in TRAM-BPTI than in BPTI, higher p^2H would be needed for the local fluctuations to become dominant, according to $(k_1^l/k_2^l)k_3 > k_1^g$. Furthermore, since the transamination of the N-terminus in TRAM-BPTI does not affect the local fluctuations (Wagner et al., 1984), similar exchange rates at high p^2H would be expected for BPTI and TRAM-BPTI. Both of these predictions are consistent with the experimental data (Figure 4, Table II). On the other hand, the deprotonation switch model could also explain the TRAM-BPTI data. In this case, however, we would have to conclude that the deprotonation of groups (tyrosines, lysines) other than the N-terminus would cause the transition to uncorrelated exchange at high pH. Otherwise, one would expect a qualitatively different behavior for TRAM-BPTI: Since TRAM-BPTI at p^2H 7 and unmodified BPTI at p^2H 9 have identical charge distributions, the onset of uncorrelated exchange at the high-p^2H end of the EX_1 plateau in TRAM-BPTI would be expected at lower p^2H than in BPTI, or the EX_1 plateau might even be completely absent in TRAM-BPTI. This has not been observed in the experiments (Figure 4).

Activation Enthalpies for Amide Proton Exchange. Recent analyses of amide proton exchange measurements relied heavily on the activation enthalpies obtained from the temperature dependence of the exchange (Woodward & Hilton, 1980; Englander & Kallenbach, 1984). It therefore appeared of interest to investigate this parameter in the presently characterized, different exchange regimes.

At suitable p^2H values, the transition from the EX_2 to the EX_1 limit can be induced by increasing the temperature. For example, for BPTI at p^2H around 8, such a transition occurs between 45 and 68 °C (Figure 7). This may have two reasons: (i) The intrinsic exchange rate, k_3, might increase more strongly with temperature than the closing rate, k_2, so that EX_1 exchange would be reached at higher temperature. (ii) The EX_2 to EX_1 transition could be due to the dominance of different classes of fluctuations at low and high temperature, i.e., global fluctuations at higher temperature with a small closing rate ($k_2^g < k_3$) and local fluctuations at lower tem-

perature with a fast closing rate ($k_2^1 > k_3$). Probably both features are relevant for the EX_2 to EX_1 transition with temperature at $p^2H \sim 8$.

Because of the potential existence of different kinetic limits, and more generally the occurrence of different classes of fluctuations, much care should be exercised in the interpretation of temperature-dependent exchange rates in terms of activation enthalpies. The apparent activation enthalpies for the two kinetic limits are

$$\Delta H^{\ddagger}_{app,EX_1} = \Delta H^{\ddagger}_{k_1} \quad (16)$$

and

$$\Delta H^{\ddagger}_{app,EX_2} = \Delta H^{\ddagger}_{k_1} - \Delta H^{\ddagger}_{k_2} + \Delta H^{\ddagger}_{k_3} \quad (17)$$

From the available literature data, the closing rates, k_2, appear to have smaller temperature dependences than the intrinsic exchange rates, k_3 (Pohl, 1976; Roder, 1981; Englander & Kallenbach, 1983). Thus, for predetermined, single type of fluctuations, we expect that

$$\Delta H^{\ddagger}_{app,EX_2} > \Delta H^{\ddagger}_{app,EX_1} \quad (18)$$

This is consistent with the experimental high-temperature values of $\Delta H^{\ddagger}_{app}$ at p^2H 3.5 (EX_2) being larger than those at p^2H 8.0 (EX_1) (Table I), keeping in mind that the exchange at both p^2H values originates from global fluctuations but corresponds to different kinetic limits.

It is interesting to consider the experimental activation enthalpies in light of the equilibrium enthalpy difference, ΔH, for the denaturation of BPTI. Moses & Hinz (1980) have measured calorimetrically a ΔH value of 70 kcal M^{-1} at the denaturation temperature, and they found this value to be independent of pH. It deviates from the much larger value reported previously by Privalov (1979). After subtracting $\Delta H^{\ddagger}_{k_3}$ = 17 kcal M^{-1} (Englander & Poulsen, 1969) from $\Delta H^{\ddagger}_{app}$ at p^2H 3.5 in Table I, we obtain opening enthalpies that are very close to ΔH for global denaturation. This suggests that at elevated temperature exchange is promoted by global unfolding transitions. From analysis of the data for the EX_1 limit at p^2H 8.0 using ΔH = 70 kcal M^{-1}, we find that $\Delta H^{\ddagger}_{k_2} \approx$ 7–11 kcal M^{-1}. These parameters are consistent with typical values reported in the literature (Englander & Kallenbach, 1984; Roder, 1981; Englander et al., 1972).

Woodward and co-workers (Woodward & Hilton, 1979, 1980; Hilton et al., 1981; Simon et al., 1984) previously interpreted the amide proton exchange in BPTI with a model involving two distinct processes: (a) a high activation energy process associated with global unfolding (dominant at low pH and elevated temperature); (b) a low activation energy process which they associated with "exchange from the folded state". Process b was invoked to explain the exchange behavior at basic pH. The distinction of processes a and b was based on the temperature dependence of exchange (Woodward & Hilton, 1980) and total hydrogen–tritium exchange measurements (Woodward et al., 1981) which indicated that protons with low activation energy were not accelerated by addition of 8 M urea. With respect to the temperature dependence, our present measurements show that some amide protons exchange by a high activation enthalpy process even at p^2H 10.9 (Figure 5; Table I) where the two-process model would predict low activation enthalpy.

While our present interpretation of BPTI exchange data agrees with some aspects of the two-process model of the Woodward group (e.g., the global nature of the high actication energy process), it differs fundamentally in other aspects: We attribute the complicated pH dependence of BPTI exchange to the fact that different parts of the distribution of internal motion are sampled as the time window of the measurement, determined by the p^2H-dependent intrinsic exchange rates, is varied. Some protons in the core of the molecule are exchanged by major unfolding transitions under all conditions presently explored. Their exchange behavior at basic pH reflects the pH dependence of unfolding. In the view of Woodward et al. (1982), exchange in the low activation energy regime is attributed to an inherently different mechanism. Exchange is believed to occur within the more or less fully folded structure after penetration of the catalyst (H_3O^+ or OH^-). In contrast, Englander & Kallenbach (1984) stress that while access of the solvent is certainly necessary, it is not sufficient for exchange to occur. Existing internal hydrogen bonds have to be disrupted, which probably involves significant structural distortion. This problem and the conceptual difficulties associated with penetration of the charged and hydrated catalysts into the protein interior are avoided by the structural unfolding model.

ACKNOWLEDGMENTS

H.R. thanks Dr. S. W. Englander for stimulating discussions on the subject of this paper. We acknowledge the careful preparation of the figures and the manuscript by E. H. Hunziker, E. Huber, and R. Marani.

Registry No. BPTI, 9087-70-1; H_2, 1333-74-0.

REFERENCES

Anil Kumar, Wagner, G., Ernst, R. R., & Wüthrich, K. (1981) *J. Am. Chem. Soc. 103*, 3654–3658.

Barksdale, A. D., & Rosenberg, A. (1982) *Methods Biochem. Anal. 28*, 1–113.

Brown, L. R., DeMarco, A., Richarz, R., Wagner, G., & Wüthrich, K. (1978) *Eur. J. Biochem. 88*, 87–95.

Covington, A. K., Robinson, R. A., & Bates, R. G. (1966) *J. Phys. Chem. 70*, 3820–3824.

Deisenhofer, J., & Steigemann, W. (1975) *Acta Crystallogr., Sect. B: Struct. Crystallogr. Cryst. Chem. B31*, 238–250.

Dixon, H. B. F., & Fields, R. (1972) *Methods Enzymol. 25*, 409–419.

Dubs, A., Wagner, G., & Wüthrich, K. (1979) *Biochim. Biophys. Acta 577*, 177–194.

Englander, S. W., & Poulsen, A. (1969) *Biopolymers 7*, 379–393.

Englander, S. W., & Kallenbach, N. R. (1984) *Q. Rev. Biophys. 16*, 521–655.

Englander, S. W., Downer, N. W., & Teitelbaum, H. (1972) *Annu. Rev. Biochem. 41*, 903–924.

Englander, S. W., Calhoun, D. B., Englander, J. J., Kallenbach, N. R., Liem, R. K. H., Malin, E. L., Mandal, C., & Rogero, J. R. (1980) *Biophys. J. 32*, 577–589.

Gurd, F. R. N., & Rothgeb, T. M. (1979) *Adv. Protein Chem. 33*, 74–165.

Hilton, B. D., & Woodward, C. K. (1978) *Biochemistry 17*, 3325–3332.

Hilton, B. D., & Woodward, C. K. (1979) *Biochemistry 18*, 5834–5841.

Hilton, B. D., Trudeau, K., & Woodward, C. K. (1981) *Biochemistry 20*, 4697–4703.

Hvidt, A., & Nielsen, S. O. (1966) *Adv. Protein Chem. 21*, 287–386.

Kabsch, W., & Sander, C. (1983) *Biopolymers 22*, 2577–2637.

Masson, A., & Wüthrich, K. (1973) *FEBS Lett. 31*, 114–118.

Molday, R. S., Englander, S. W., & Kallen, R. G. (1972) *Biochemistry 11*, 150–158.

Moses, E., & Hinz, H.-J. (1983) *J. Mol. Biol. 170*, 765–776.
Pohl, F. M. (1976) *FEBS Lett. 65*, 293–296.
Privalov, P. L. (1979) *Adv. Protein Chem. 33*, 167–241.
Richarz, R., & Wüthrich, K. (1978) *J. Magn. Reson. 30*, 147–150.
Richarz, R., Sehr, P., Wagner, G., & Wüthrich, K. (1979) *J. Mol. Biol. 130*, 19–30.
Roder, H. (1981) Ph.D. Thesis, ETH Zürich.
Roder, H., Wagner, G., & Wüthrich, K. (1985) *Biochemistry* (following paper in this issue).
Simon, I., Tüchsen, E., & Woodward, C. (1984) *Biochemistry 23*, 2064–2068.
Stassinopoulou, C. I., Wagner, G., & Wüthrich, K. (1984) *Eur. J. Biochem. 145*, 423–430.
Štrop, P., Wider, G., & Wüthrich, K. (1983) *J. Mol. Biol. 166*, 641–667.
Wagner, G. (1980) *Biochem. Biophys. Res. Commun. 97*, 614–620.
Wagner, G. (1983) *Q. Rev. Biophys. 16*, 1–57.
Wagner, G., & Wüthrich, K. (1979a) *J. Mol. Biol. 134*, 75–94.
Wagner, G., & Wüthrich, K. (1979b) *J. Magn. Reson. 33*, 675–680.
Wagner, G., & Wüthrich, K. (1982a) *J. Mol. Biol. 155*, 347–366.
Wagner, G., & Wüthrich, K. (1982b) *J. Mol. Biol. 160*, 343–361.
Wagner, G., Tschesche, H., & Wüthrich, K. (1979) *Eur. J. Biochem. 95*, 239–248.
Wagner, G., Stassinopoulou, C. I., & Wüthrich, K. (1984) *Eur. J. Biochem. 145*, 431–436.
Woodward, C. K., & Hilton, B. D. (1979) *Annu. Rev. Biophys. Bioeng. 8*, 99–127.
Woodward, C. K., & Hilton, B. D. (1980) *Biophys. J. 32*, 561–575.
Woodward, C. K., Simon, I., & Tuchsen, E. (1982) *Mol. Cell. Biochem. 48*, 135–160.
Wüthrich, K., & Wagner, G. (1979) *J. Mol. Biol. 130*, 1–18.
Wüthrich, K., & Wagner, G. (1982) *Ciba Found. Symp. 93*, 310–328.
Wüthrich, K., & Wagner, G. (1984) *Trends Biochem. Sci. (Pers. Ed.) 9*, 152–154.
Wüthrich, K., Eugster, A., & Wagner, G. (1980) *J. Mol. Biol. 144*, 601–604.
Wüthrich, K., Štrop, P., Ebina, S., & Williamson, M. P. (1984) *Biochem. Biophys. Res. Commun. 122*, 1174–1178.

Individual Amide Proton Exchange Rates in Thermally Unfolded Basic Pancreatic Trypsin Inhibitor†

Heinrich Roder,‡ Gerhard Wagner,* and Kurt Wüthrich
Institut für Molekularbiologie und Biophysik, Eidgenössische Technische Hochschule, Zürich-Hönggerberg, CH-8093 Zürich, Switzerland

Received December 20, 1984

ABSTRACT: A novel experiment is described for measurements of amide proton exchange rates in proteins with a time resolution of about 1 s. A flow apparatus was used to expose protein solutions in ^2H_2O first to high temperature for a predetermined time period, during which ^1H–^2H exchange proceeded, and then to ice–water. The technique was applied for exchange studies in thermally unfolded, selectively reduced basic pancreatic trypsin inhibitor. Measurements were made by ^1H nuclear magnetic resonance after the exchange was quenched by rapid cooling. Thereby, the sequence-specific resonance assignments for the folded protein could be used, which had been previously obtained. The results of this study indicate that the exchange rates in the thermally unfolded protein are close to those expected for a random chain and that the NH exchange is catalyzed by $^2H^+$ and O^2H^- up to high temperature, with no significant contributions from p^{2}H-independent catalysis. We conclude that the parameters derived by Molday et al. [Molday, R. S., Englander, S. W., & Kallen, R. G. (1972) *Biochemistry 11*, 150–158] from measurements with small model peptides can be used to calculate intrinsic exchange rates in unfolded proteins and thus provide a reliable reference for the interpretation of exchange rates measured under native conditions.

Measurements of exchange rates of interior labile protons are a widely used method for investigating internal motility in globular proteins (Linderstrøm-Lang, 1955; Hvidt & Nielsen, 1966; Englander et al., 1972; Wagner & Wüthrich, 1979a). Usually the data are evaluated on the basis of a structural unfolding model:

$$N(H) \underset{k_2}{\overset{k_1}{\rightleftharpoons}} O(H) \xrightarrow[^2H_2O]{k_3} O(^2H) \underset{k_1}{\overset{k_2}{\rightleftharpoons}} N(^2H) \qquad (1)$$

N indicates the ensemble of "closed" conformers in which the labile proton considered is not accessible to the deuterated solvent (for example, because of internal hydrogen bonding). O indicates the "open" conformers in which the same proton is in contact with the solvent. k_1 and k_2 describe the rates of interchange between closed and open states of the protein, and k_3 is the intrinsic exchange rate for the solvent-accessible, labile proton. Depending on the ratios of these rate constants, different limiting kinetic situations may arise (Hvidt & Nielsen, 1966). However, the experimental observations presented in the preceding paper (Roder et al., 1985) indicate that for studies of the exchange of interior backbone amide protons in proteins, exchange via an EX_2 mechanism will

† This work was supported by the Swiss National Science Foundation (Projects 3.528.79 and 3.284.82).
‡ Present address: Department of Biochemistry and Biophysics, University of Pennsylvania School of Medicine, Philadelphia, PA 19104.

0006-2960/85/0424-7407$01.50/0